A Compact and Systematic Design of Microstrip and Suspended Stripline Structure (SSS) Bandpass Filter with Defected Structure for Wideband Applications

Z. Zakaria[1], M. A. Mutalib[2], A. B. Jiim
Centre for Telecommunication Research & Innovation (CeTRI),
Faculty of Electronic & Computer Engineering,
Universiti Teknikal Malaysia Melaka (UTeM), Hang Tuah Jaya,
76100, Durian Tunggal, Melaka, Malaysia.
[1]zahriladha@utem.edu.my, [2]ariffinmutalib@gmail.com

Abstract: - This paper presents the design of microstrip and suspended stripline structure microwave filter with defected structure to produce a bandpass and notch response simultaneously in a single structure. The first design was microstrip Chebyshev bandpass filter integrated with defected microstrip structure (DMS) using λ_{g0} short-circuited stubs structures of 7th degree. While, the suspended stripline structure was design using cascaded method of generalized Chebyshev lowpass and highpass to produce bandpass filter. This bandpass filter was integrated with defected stripline structure (DSS) to remove the unwanted signal simultaneously. The bandpass filter was designed at wideband frequency from 3 GHz to 6 GHz with a fractional bandwidth of 66.7%. The integration of bandpass filter with defected structure produced high selectivity and attenuation of notch response at resonant frequency of 5.2 GHz and *Q*-factor is better than 34.67. The design was simulated and fabricated on a Roger Duroid RO4350 with a dielectric constant, ε_r of 3.48 and a thickness of 0.508 mm. The experimental results show good agreement and are in-line with the simulated performance. This new class of generalized Chebyshev bandpass filter with DSS is useful to remove any undesired signal in any wideband communication system, particularly in civilian and military radar applications.

Key-Words: - Chebyshev, generalized Chebyshev, bandpass filter, *Q*-factor, transmission zeros

1 Introduction

The demand for new designs and approaches of microwave filter is increasing and intensively investigated. Some recent work on this subject has demonstrated the techniques that are used to synthesize the bandpass filter using the Chebyshev response. For example, multi-mode resonator to form a UWB bandpass filter [1], quarter-wavelength and half-wavelength to constitute a narrow bandpass filter [2]-[4], and many other types of resonators [5]-[7].

The design bandpass filter by [8] proposed the embedding of individually design highpass structure and lowpass filter into each other. But this method has to control the high- and low-Z section between stubs element. It will disturb the intersection between the two impedances.

The structure design by [9] composed of a stepped impedance parallel-coupled Microstrip line structure. However, by using DGS, the ground plane start radiates the electromagnetic wave, which interfere the nearby circuitry of the system. The optimization short circuited stub was designed by [10]. This work attempted to develop a compact high-selectivity UWB bandpass filter with about 110% fractional bandwidth. However, the suppression occurs at the higher frequency that will disturb other frequency band. In other research by [11] based on the design of UWB suspended substrate stripline highpass filter, this design of highpass filter has a cut-off frequency of 4 GHz. However, the tight coupling on the top and bottom stripline is difficult to control to produce better selectivity. In [12], the researchers used another technique to remove the unwanted signals using a parasitic coupled line embedded with a compact microstrip bandpass filter. However, this method has suppression at higher frequencies, and will disturb the selectivity of the response.

In this paper, an integrated microstrip and suspended stripline structure with defected structure to produce a new class and compact design of microwave filter to exhibit bandpass and notch response simultaneously. The filter is designed at a centre frequency of 4.5 GHz with minimum stopband insertion loss of 40 dB and minimum passband return loss of 15 dB. This type of filter is useful in any RF/ microwave communication systems particularly to eliminate any undesired signals in wideband spectrum. While maintaining its

excellent performance, the overall physical and cost reduction can also be achieved using this technique.

2 Microwave Filter Design Procedure

Microwave filters can be systematically designed starting from lowpass prototype and normally have a system impedance of 1 Ω. The prototype element can be presented as a lumped element or distributed realization which some transformation is needed before it can be used to convert to lowpass, bandpass and bandstop with arbitrary centre frequency and bandwidth. Moreover, there are several types of filter response that can be realized such as Chebyshev and generalized Chebyshev [13].

The advantage of the generalized Chebyshev compared to Chebyshev response is that the generalized Chebyshev can achieve higher selectivity and low losses compared to the Chebyshev response. This is because the transmission zeros can be placed in the arbitrary frequency response. Furthermore, the generalized Chebyshev can reduce the number of orders and also the number of elements [14].

The lumped element is then converted to distributed element using the Richard's Transformation technique. Basically, the design of a filter is based on some approximate equivalence between lumped and distributed elements, which can be established by applying this method. This implies that the distributed circuits composed of equal-length open- and short-circuited transformation lines can be created as lumped elements under the transformation. Richard's transformation allows us to replace lumped inductors with short-circuited stubs of characteristic impedance $Z_0 = L$ and capacitors with open-circuited stubs of characteristic impedance, $Z_0 = 1/C$. The transformation of lumped element to stub element.

3 Microstrip Bandpass Filter Design

The design of bandpass filter is started from lowpass prototype element; g_1=g_7=1.1812, g_2=g_6=1.4228, g_3=g_5=2.0967, g_4 =1.5734. To design the lowpass prototype filter the following specification should be identified. The lowpass prototype filter with centre frequency of 4.5 GHz with the degree, N=7, the minimum stpband insertion loss of better than 40 dB and minimum passband return loss of better than 20 dB are designed. This prototype element is used in conventional microstrip bandpass filter which is $\lambda_{g0}/4$ short-circuited stub. The bandpass filter is designed using shunt short-circuited stubs which are $\lambda_{g0}/4$ long with connecting lines that are also $\lambda_{g0}/4$ long as shown in Fig. 1.

The design equation for determining these characteristics admittance described in [15].

$$\theta = \frac{\pi}{2}\left(1 - \frac{FBW}{2}\right) \quad (1)$$

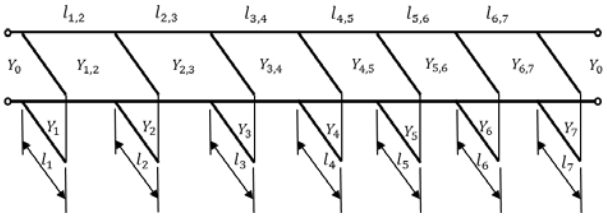

Fig. 1. Modeling circuit of the proposed wideband bandpass filter

The bandpass filter was designed to have a fractional bandwidth (*FBW*) of 66.67% at a mid-band frequency, f_o=4.5 GHz. A 50 Ω impedance is chosen which give Y_o=1/50 mhos. The parameter design can be calculated using the following equations. The stub length and separation depend on characteristics admittances, Y_i and transmission line admittance, $Y_{i,i+1}$. The transmission line admittance, $Y_{i,i+1}$ can be obtained by using equation in [15]:

Based on equation in [15], the line impedance of each stub and connecting line in Fig. 1 can be calculated as follows: $Z_1 = Z_7 = 44.32\ \Omega$, $Z_2 = Z_6 = 22.52\ \Omega$, $Z_3 = Z_5 = 22.58\ \Omega$, Z_4=22.27 Ω, $Z_{1,2} = Z_{6,7} = 38.81\ \Omega$, $Z_{2,3} = Z_{5,6}$=36.56 Ω, $Z_{3,4} = Z_{4,5} = 38.45\ \Omega$. The filter design was based on a circuit model for 7th order stub bandpass filter with quarter-wavelength short-circuited stubs.

The characteristic impedances of the short-circuited stubs are defined by Z_1 to Z_7, and the characteristic impedances for the connecting lines are defined by $Z_{1,2}$ to $Z_{6,7}$. The design of the filter is implemented using microstrip on the Roger Duroid RO4350 substrate (ε_r=3.48, $tan\delta$=0.0019, and thickness = 0.508 mm). The calculated admittances and impedances for seven short-circuited stubs (Y_i and Z_i) and transmission lines ($Y_{i,i+1}$ and $Z_{i,i+1}$) are applied to standard equation for microstrip design described in [15]. The widths, *W* and guided quarter-wavelength, λ_{g0} associated with the characteristic admittances can be found and are listed in Table 1.

The physical layout and dimensions of the optimized short circuited stubs bandpass filter is shown in Fig. 2. The comparison of current flow visualization of the physical layout is shown in Fig. 3 (a), (b) and (c) representatively

Table 1: Microstrip design parameters of 7th order stub bandpass filter

i	W_i (mm)	$\lambda_{g0i}/4$ (mm)	$W_{i,i+1}$ (mm)	$\lambda_{g0i,i+1}/4$ (mm)
1	1.3918	10.00	1.69	9.928
2	3.4926	9.64	1.8406	9.845
3	3.4922	9.64	1.7136	9.923
4	3.5184	9.64	1.7136	9.923
5	3.4922	9.64	1.8406	9.845
6	3.4926	9.64	1.69	9.928
7	1.3818	10.00	-	-

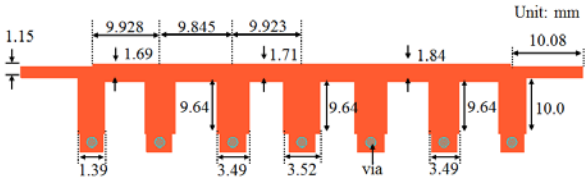

Fig. 2. Layout of the Microstrip bandpass filter

In Fig. 3 (a), the current visualization flow focuses at frequency 3 GHz. The response has more concentration at the stubs of the physical layout. Fig. 3 (b), shows the current visualization flow for frequency at 4.5 GHz and Fig. 3 (c) shows the current visualization flow for frequency at 6.0 GHz. In this figure, the current flow visualization is concentrated on the connecting lines of the physical layout.

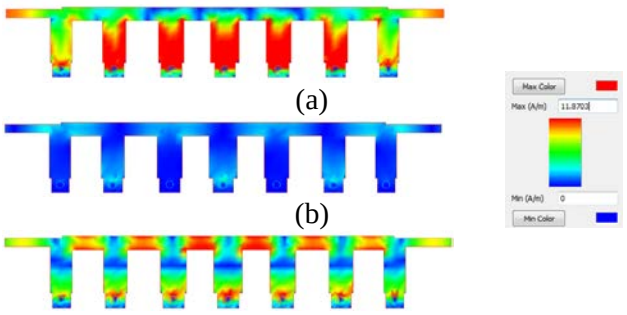

Fig. 3. Current flow visualization of short circuit stubs bandpass filter (a) at 3 GHz, (b) at 4.5 GHz and (c) at 6 GHz

The structure of bandpass filter consists of microstrip line on the top of the substrate and ground plane at the bottom of the substrate. Via hole represents short circuit stubs connecting the microstrip line and the ground plane. Fig. 4 shows that the fabricated of short circuited stubs bandpass filter design. The experimental results show good agreement and are in-line with the simulated performance. In the experimental results, the centre frequency of 4.5 GHz with a return loss and insertion loss is better than 10 dB and better than 0.2 dB respectively. Then fractional bandwidth of around 69.5% was measured as shown in Fig. 5. Fig. 6 shows the group delay for the bandpass filter is very flat in the passband, lower than 0.71 ns for simulated response while for the measured response the group delay is 0.98 ns.

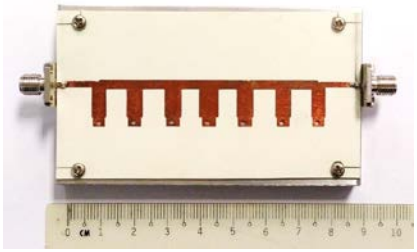

Fig. 4. The fabricated of short circuit stubs bandpass filter

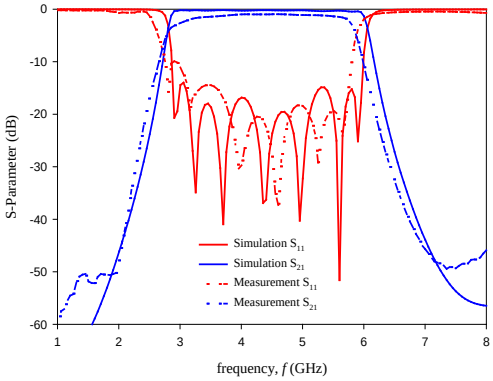

Fig. 5. Comparison between simulated and measured response short circuited stubs bandpass filter

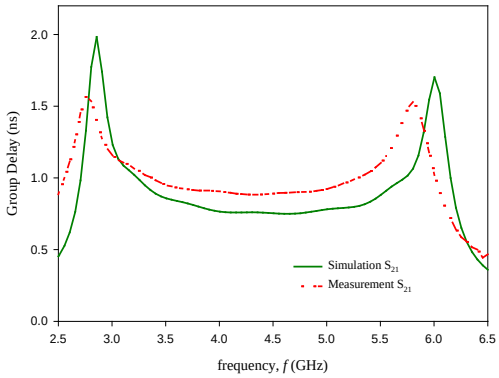

Fig. 6. Comparison group delay between simulated and measured response of short circuited stubs bandpass filter

4 Suspended Stripline Structure (SSS) Bandpass Filter Design

The generalized Chebyshev filter has equiripple response in passband but with arbitrarily placed transmission zeros in the stopband offering selectivity nearly as good as the elliptic filter of the same degree. From this point of view, the

ISBN: 978-1-61804-302-3

generalized Chebyshev filter prototype is more preferred due to the transmission zeros that can be placed independently in accordance to design specification.

In terms of number of degree, for a particular specification, elliptic filter gives the least number of elements which results in circuit size reduction. As an example, for a wideband bandpass filter with the stopband insertion loss of 50 dB, the passband return loss of 20 dB and selectivity of 2, a Butterworth filter require twelve numbers of elements while Chebyshev filter needs only seven.

4.1 Generalized Chebyshev Lowpass Filter

To design the lowpass filter, the prototype lowpass filter should be identified by the following specification. The lowpass filter with cut-off frequency of 6 GHz with the degree, N=7, the minimum stpband insertion loss of better than 40 dB and minimum passband return loss of better than 20 dB are designed. The elements values for the lowpass prototype network are; C_1 =C_7 = 1.02647, C_3 = C_5 = 1.10006, L_2 = L_6 = 1.08027, L_3 = L_5 = 0.541922 and L_4 = 0.984147.

The lowpass prototype operates in system impedance of 1Ω and cut-off frequency of 1 rad/s. The next step is to perform the transformation to lowpass filter with 50 Ω from the lowpass prototype using following equations in [16]. The values of each capacitor and inductors that operating in 50 Ω impedance, with cut-off frequency of 6 GHz can be calculated. The element values of the equivalent circuit for lowpass filter are; C_1 =C_7 = 0.545 pF, C_3 = C_5 = 0.584 pF, L_2 = L_6 = 1.433 nH, L_3 = L_5 = 0.719 nH and L_4 = 1.305 nH. The lowpass filter circuit can now be seen in Fig. 7.

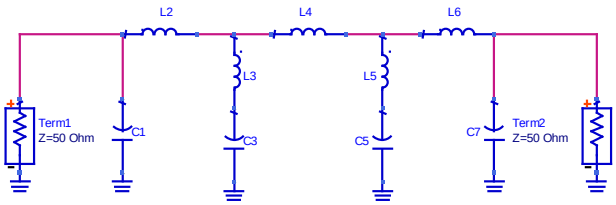

Fig. 7. Equivalent circuit of the 7th order generalized Chebyshev lowpass filter

For realization, the lumped element lowpass filter is then transformed to open- and short-circuit transmission line segments by applying Richard's transformation [17]. The Richard's transformation allows to replace lumped inductors with short circuited stubs of characteristic impedance $Z_o = L$ and capacitors with open circuited stubs of characteristic impedance, $Z_o = 1/C$. The resonator impedance can be represented as admittance of an open circuited stub by characteristic admittance $\alpha\, C/2$. The length of the stub is one quarter wavelength at ω_0. Constant a can be obtained by applying Richard's transformation at the band-edge frequency ω_c.

The structure of distributed element after applying the Richard's transformation is shown in Fig. 8. The values of short- and open-circuit stubs are; Z_{SC1} = Z_{SC2} = Z_{SC3} = 120 Ω, E_{SC1} = E_{SC2} = E_{SC3} = 29.9°, Z_{OC1} = Z_{OC4} = 29.78 Ω, E_{OC1} = E_{OC4} = 29.127°, Z_{OC2} = Z_{OC3} = 55.55 Ω, E_{OC2} = E_{OC3} = 72°. Fig. 9 shows the current flow visualization of generalized Chebyshev lowpass filter at 6.0 GHz. Red color means strong density and concentrated electric field with 15.42 A/m. Since the simulated conductor is a perfect conductor, all electrons are at the conductor surface. The blue color means there is less electric field inside the conductor.

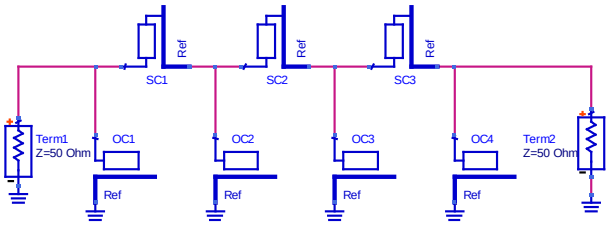

Fig. 8. Distributed element of lowpass filter

Fig. 9. Current flow visualization of generalized Chebyshev lowpass filter at 6 GHz

Fig. 10 shows the simulated insertion loss and return loss of the generalized Chebyshev lowpass filter. The filter has a cut-off frequency of 6.0 GHz, with very good matching at the passband and the return loss is better than 18 dB. There are two transmissions zero occurring at 6.5 GHz and 7.5 GHz during the process of optimizing the stubs.

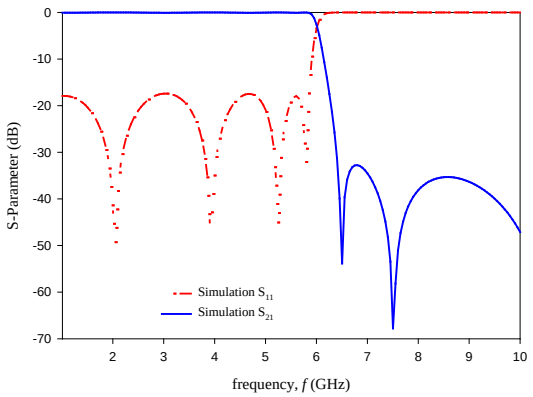

Fig. 10. Simulated response of physical layout a generalized Chebyshev lowpass filter

ISBN: 978-1-61804-302-3

4.2 Generalized Chebyshev Highpass Filter

In designing the highpass filter, the lowpass filter prototype will be transformed into a highpass filter with an arbitrary cutoff frequency. However, this work chose the dual type generalized Chebyshev lowpass prototype filter instead of the one used for the lowpass filter design described earlier in Section 4.1. The dual type of lowpass prototype network which satisfies a generalized Chebyshev response having three transmission zeros at infinity and (*N*-3) at a finite frequency.

The transformation from lowpass prototype to arbitrary highpass filter with specific cut-off frequency can be found using the equation (2);

$$\omega \rightarrow \frac{-\omega_c}{\omega} \tag{2}$$

where ω_c is cutoff frequency

This maps the lowpass filter prototype cutoff frequency to a new frequency. The transformation is applied to inductors and capacitors. Hence the inductors are transformed into capacitors and capacitors are transformed into inductors as shown in Fig. 11. The element values of the equivalent circuit for highpass filter are; C_1 =C_7 = 1.0003 pF, C_3 = C_5 = 1.0261 pF, L_2 = L_6 = 2.3763 nH, L_3 = L_5 = 4.7368 nH and L_4 = 2.6084 nH.

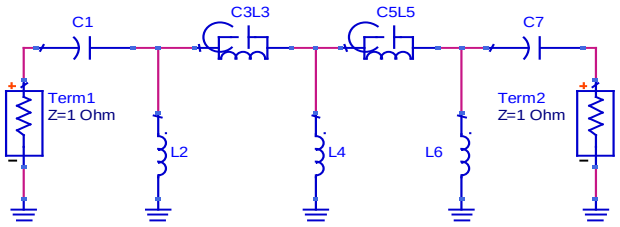

Fig. 11. Equivalent circuit of the 7th order generalized Chebyshev highpass filter

Generalized Chebyshev highpass filter in distributed form can be constructed by applying Richard's transformation to the highpass filter prototype. Under this transformation, inductors were transformed into short circuits with impedance and capacitors into open circuits with admittance. Following the Richard's transformation, length for all the stubs was varied uniformly to obtain a sufficiently wide passband and good rejection in the stopband for the bandpass filter once the lowpass filter was cascaded with the highpass filter.

The structure of distributed element after applying the Richard's transformation is shown in Fig. 12. The values of short- and open-circuit stubs are; Z_{OC1} = Z_{OC7} = 29.4 Ω, E_{OC1} = E_{OC7} = 30°, Z_{OC3} = Z_{OC5} = 42.12 Ω, E_{OC3} = E_{OC5} = 30°, Z_{SC2} = Z_{SC6} = 70.05 Ω, E_{SC2} = E_{SC6} = 30°, Z_{SC3} = Z_{SC5} = 338 Ω, E_{SC3} = E_{SC5} = 30°, Z_{SC4} = 69.3 Ω, E_{SC4} = 30°.

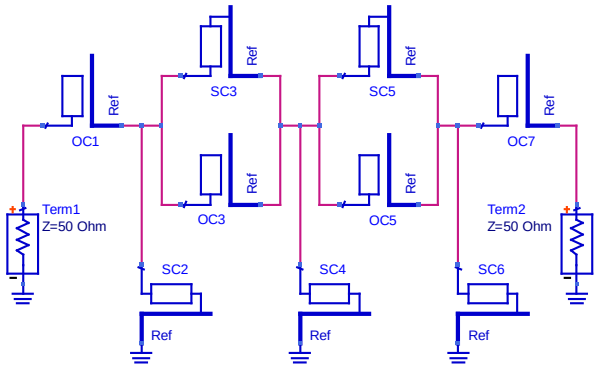

Fig. 12. Distributed element of highpass filter

Fig. 13 shows the current flow visualization of generalized Chebyshev highpass filter at 3 GHz. Red color means strong density and concentrated electric field. Since the simulated conductor is a perfect conductor, all electrons are at the conductor surface. The blue color means there is less electric field inside the conductor. Fig. 14 shows the simulated insertion loss and return loss of the generalized Chebyshev highpass filter. The filter has a cut-off frequency of 3 GHz, with very good matching at the passband and the return loss is better than 15 dB. At about 2.4 GHz a transmission zero occurred due to the coupling effect between each stubs and the coupling effect from the top and bottom layers. By carefully selecting the electrical length of the stubs, a broader passband can be obtained. In this research, an electrical length of 30° was chosen due to good rejection in the stopband. In order to realize the highpass filter layout, series capacitors and resonators can be approximated by inhomogeneous couple lines realized in suspended substrate.

The generalized Chebyshev bandpass filter can be realized by cascading lowpass filter in Fig. 7 and highpass filter in Fig. 11. Fig. 15 shows the cascading generalized Chebyshev bandpass filter circuit. The suspended stripline structure as shown in Fig. 16 is one of the best method for physically realizing the filter. This SSS consists of a thin printed circuit suspended between parallel ground planes [17].

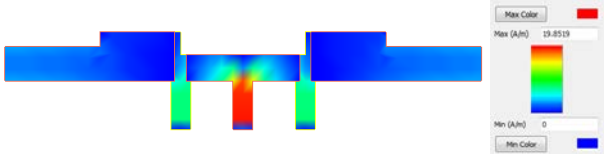

Fig. 13. Current flow visualization of generalized Chebyshev highpass filter at 3 GHz

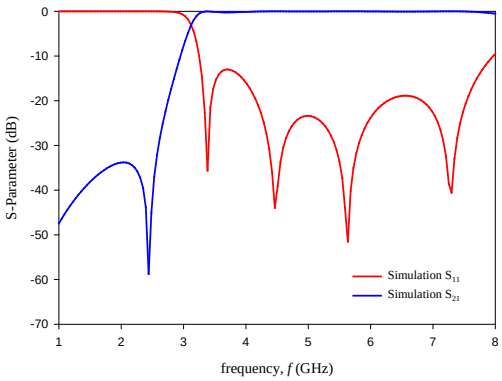

Fig. 14. Simulated response of physical layout generalized Chebyshev highpass filter

The majority of the field of the suspended stripline structure is in the air and the substrate has a small effect on the *Q*-factor or the effective permittivity of the elements. It is relatively straightforward to calculate the dimensions of the individual circuit element within the filter. Consider a single transmission line of width, *w* and thickness, *t* suspended between ground planes with spacing, *b*.

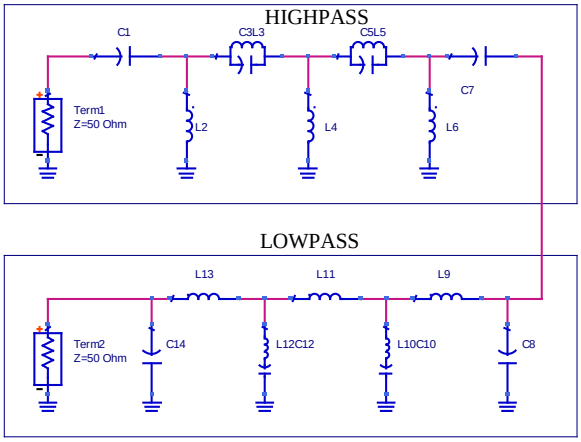

Fig. 15. Equivalent circuited of the generalized Chebyshev bandpass filter

The impedance of the SSS which is based on Tranverse Electromagnetic (TEM) transmission line is related to its static capacitance to ground per unit length as the following:

$$Z_0\sqrt{\varepsilon_r} = \frac{377}{C/\varepsilon} \tag{3}$$

where ε_r is the dielectric constant of the medium and C/ε is the normalized static capacitance per unit length of the transmission line. If a transmission line is suspended, the normalized static capacitance would include fringing capacitance.

In order to realize the highpass filter layout, series capacitors and resonators can be approximated by inhomogeneous couple lined realized in suspended substrate. A series capacitance can be realized in the form of parallel coupled structure, overlapping of strips on the top and bottom layers of the substrate.

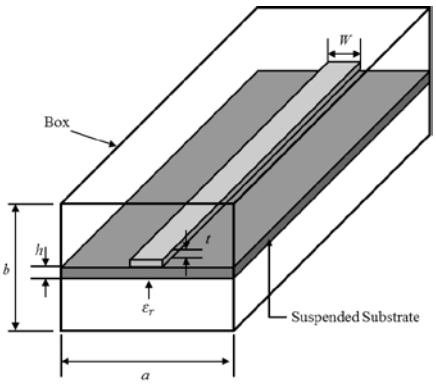

Fig. 16. Perspective view of suspended stripline structure

To produce a wider bandwidth, the value of necessary impedance became too small to fabricate effect of line separation. This limitation can overcome in suspended stripline where the larger impedance can be produced by using broadside-couple lines.

$$Z_0 = \frac{\eta_o}{\sqrt{\varepsilon_e}}\left[\frac{w}{h} + 1.393 + 0.667\ \ln\left(\frac{w}{h} + 1.444\right)\right]^{-1} \tag{4}$$

where

$$\varepsilon_e = \frac{1}{2}\left[\varepsilon_r + 1 + (\varepsilon_r - 1)F\right] \tag{5}$$

and

$$F = \left(1 + \frac{12h}{w}\right)^{-1/2} \tag{6}$$

ε_r is the relative dielectric constant of substrate and η_0 is the wave impedance which is 377 Ω.
The series capacitors are represented by an overlapping line possessing capacitance C_S. The length overlaps is given by

$$l = \frac{1.8\, u\, Z_{oo}\, C_s}{\sqrt{\varepsilon_e}} \tag{7}$$

where u is the phase velocity and Z_{oo} is the odd mode impedance and is given by replacing h in (4) by $h/2$. For the series resonators, the capacitance too can be represented by the length of overlapping lines and can be calculated from (4) and (7). The nearer distance between them means tighter coupling results in a better selectivity.

Hence, by cascading them, small and flat group delay can be achieved for wideband bandpass filter. This cascade introduces new $\lambda/2$ line impedance in

ISBN: 978-1-61804-302-3

order to maintain a good appropriate response of the S-parameter as shown in Fig. 17. This method can reduce the overall size of the bandpass filter as well as to maintain a good output of the filter. This physical layout is the optimized dimension during the simulation on transmission line suspended stripline structure in order to satisfy the desired responses. The structure of the bandpass filter was covered with an aluminium box represented as conducting housing or ground planes.

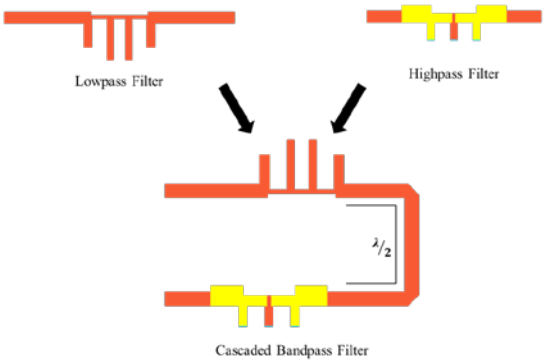

Fig. 17. Physical layout of the 7th order generalized Chebyshev bandpass filter

In the suspended stripline structure configuration, the majority of the fields is in the air cavity and the substrate has little effect on the *Q*-factor or the effective permittivity of the elements. Fig. 18 shows the current flow visualization of generalized Chebyshev bandpass filter at 3 GHz, 4.5 GHz and 6.0 GHz respectively. Red color means strong density and concentrated electric field with 25.92 A/m. Since the simulated conductor is a perfect conductor, all electrons are at the conductor surface. The blue color means there is less electric field inside the conductor. Fig. 19 shows the fabricated of the generalized Chebyshev bandpass filter with a final length and width dimension of 50 mm and 45 mm. This filter is then manufactured in an aluminium material using an in-house CNC milling machine.

Fig. 20 shows the comparison between the simulated and measured response. The measured (simulated) data show a passband of 3 – 6.2 GHz (3–6 GHz) with a fractional bandwidth of 66.67% (63.74%) and with a maximum in insertion loss of 0.5 dB (0.1dB) and the return loss is 17 dB (19 dB). The group delay of the generalized Chebyshev bandpass filter was measured and compared with the simulation as shown in Fig. 21. The measured group delay was found very flat in the whole passband, which is below 0.92 ns.

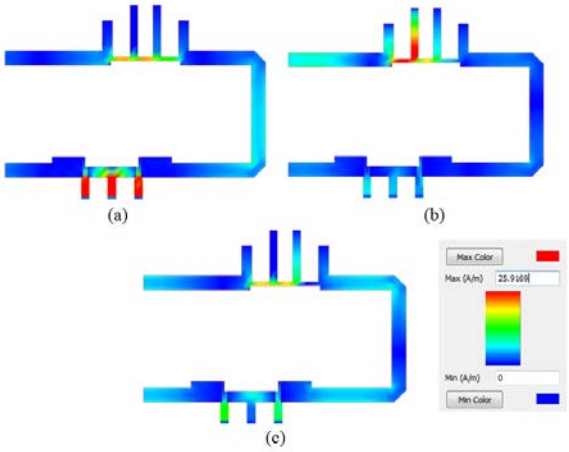

Fig. 18. Current flow visualization of generalized Chebyshev bandpass filter at (a) 3 GHz, (b) 4.5 GHz and (c) 6 GHz

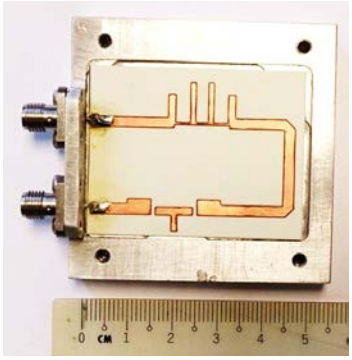

Fig. 19. The fabricated of generalized Chebyshev bandpass filter without lid

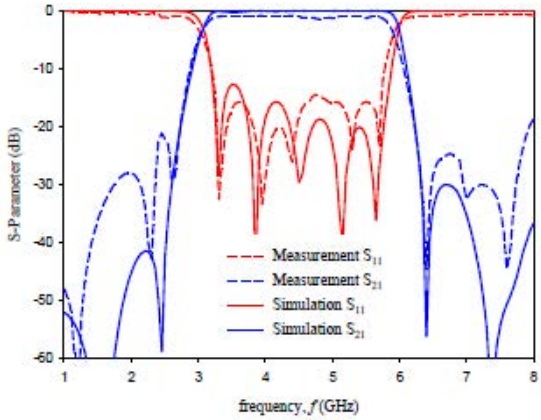

Fig. 20. Comparison of simulated and measured generalized Chebyshev bandpass filter

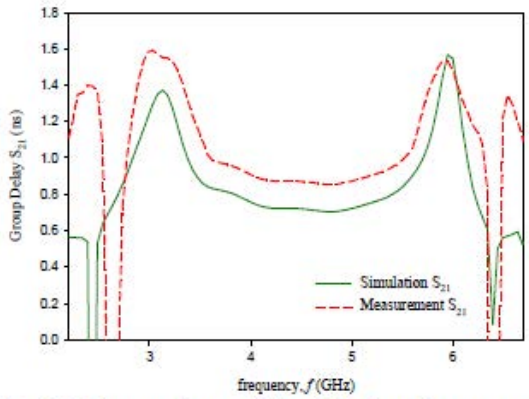

Fig. 21. Comparison of simulated and measured group delay of generalized Chebyshev bandpass filter

5 Integrated Bandpass Filter and Defected Structure

The defected structure is designed at 5.2 GHz to avoid the interferences of wireless local area network (WLAN) radio signal. The optimized geometric parameters of the microstrip structure and suspended stripline structure are used for the integration technique of defected structure. The results from the simulation of defected structure are analysed through the parametric studies in order to get the optimum results.

5.1 Microstrip Bandpass Filter with Defected Microstrip Structure

The DMS can be placed at any physical structure of microstrip transmission line to produce band reject response. Fig. 22 shows the current flow visualization of integrated bandpass filter and DMS. It is shown that the current flow focuses on DMS structure at resonant frequency of around 5.2 GHz. Fig. 23 shows the fabricated of the integrated bandpass filter and DMS structure in a finalized length and width dimension of 90 mm and 25 mm. Fig. 24 shows the comparison between the simulated and measured response of integrated bandpass filter and DMS structure.

The measured passband of frequency response was found to be 2.9 GHz to 5.8 GHz (-3dB FBW=66.67%). The return and insertion loss of this type of filter were found to be lower than 16 dB and better than 1 dB. The notch response of DMS is 5.15 GHz with the bandwidth of around 5.77%. The group delay of the wideband bandpass filter with DMS was measured and compared with that of the simulation as shown in Fig. 25. The measured group delay was found very flat in the entire band except in the notched band. The overall measured results were in good agreement with the simulations.

Fig. 22. Current flow visualization of bandpass filter integrated with DMS

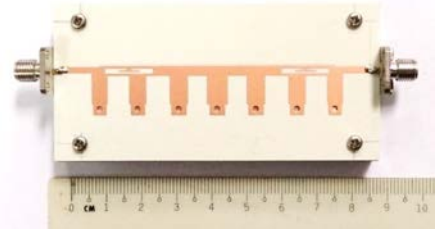

Fig. 23. The fabricated of integrated bandpass filter with inverse T-shape DMS

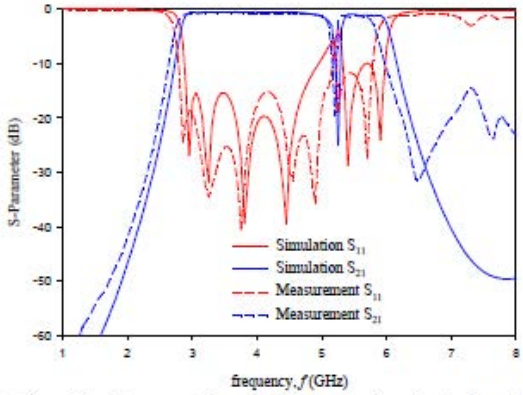

Fig. 24. Comparison between simulated and measured response of integrated bandpass filter and DMS

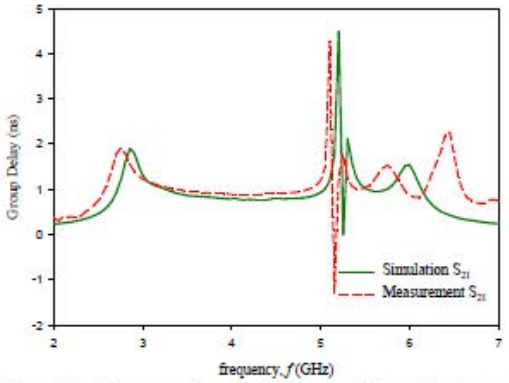

Fig. 25. Comparison of group delay between simulated and measured response of integrated bandpass filter and DMS

5.1 Suspended Stripline Structure (SSS) Bandpass Filter with Defected Microstrip Structure

The DSS was then integrated with the bandpass filter to produce bandpass and band reject responses simultaneously. The DSS was placed at the $\lambda/2$ line impedance with the specific dimension and the resonant frequency. Fig. 26 the current visualization flow focuses at frequency 3 GHz. The response has

ISBN: 978-1-61804-302-3

more concentration at the stubs of the physical layout. Fig. 26 (b), the current visualization flow focuses at a passband resonant frequency of 4.5 GHz where the connecting line of the stubs shows more concentration. Fig. 26 (c) shows the current visualization flow for the frequency of 6.0 GHz. In this figure, the current flow visualization concentrates on the DMS structure at the resonant frequency of around 5.2 GHz.

Fig. 27 shows the fabricated of the integrated bandpass filter and DSS structure with final length and width dimension of 55 mm and 50 mm. The substrate was shielded in the mount by a height of 1.0 mm over and below the substrate. The integrated bandpass filter and DSS was designed to exhibit a pure transverse electro-magnetic (TEM) mode of propagation which resulted in a very low loss characteristics and excellent selectivity.

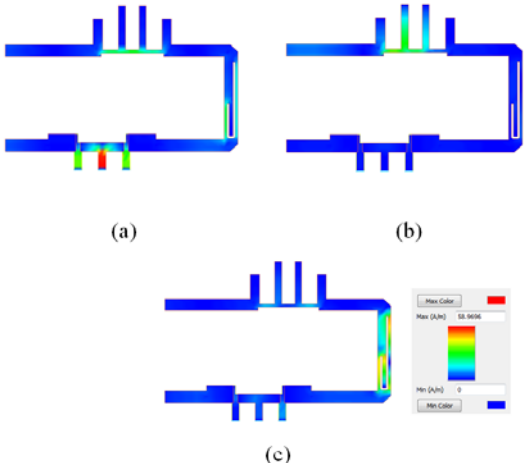

Fig. 26. Current flow visualization of integrated bandpass filter with DSS (a) at 3 GHz, (b) at 6 GHz and (c) at 5.2 GHz

Fig. 28 shows the comparison between the simulated and measured response of integrated bandpass filter with DSS structure. The measured passband covers a range from 2.9 to 6 GHz, while the measured notched band is exactly centred at 5.2 GHz with an attenuation of greater than 25 dB and the 3-dB bandwidth is about 6.73 % with *Q*-factor of 34.78. The measured group delay shows good flatness in the whole passband, except the notched response as shown in Fig. 29.

6 Conclusion

The compact design of Chebyshev and generalized Chebyshev uses microstrip structure and suspended stripline structure has been successfully designed. The bandpass is then integrated with defected structure to eliminate the unwanted signal to avoid interference with undesired signal The experimental results showed good agreement and are in-line with the simulated performance.The defected structure can be easily designed by tuning the dimension of the structure itself. Further research in reconfigurable filter design will improve the performance and also increase the functionality of the filter. This new class of Chebyshev and generalized Chebyshev response is useful in any wideband communication system particularly in civilian and military radar applications with high selectivity.

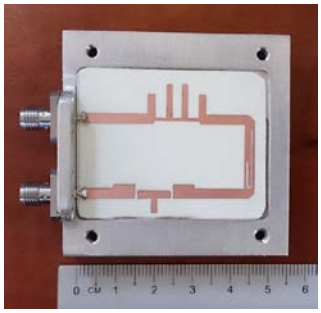

Fig. 27. The fabricated of integrated bandpass filter and J-shape DSS

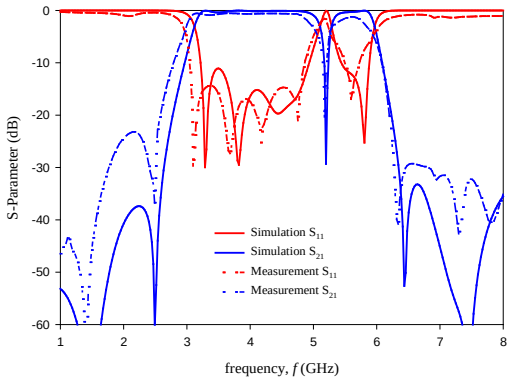

Fig. 28. Comparison between simulated and measured response of integrated bandpass filter and DSS

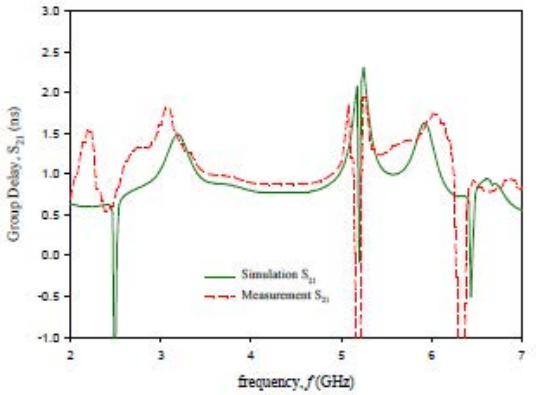

Fig. 29. Comparison group of delay between simulated and measured response of integrated bandpass filter and DSS

ISBN: 978-1-61804-302-3

Acknowledgment

The authors would like to thanks UTeM and MOSTI for sponsoring this work under the following research grants, PJP/2013/FKEKK(2B)/S01131 and MOSTI, 06-01-14-SF0103.

References:

[1] Gao, M.-J., L.-S. Wu, and J. F. Mao, "Compact Notched Ultra-Wideband Bandpass Filter with Improved Out-of-band Performance Using Quasi Electromagnetic Band Gap Structure," *Progress In Electromagnetics Research,* vol. 125, 2012, pp. 137–150,

[2] Chen, Y.-M., S.-F. Chang, C.-C. Chang, and T.-J. Hung, "Design of Stepped-Impedance Combline Bandpass Filters with Symmetric Insertion-Loss Response And Wide Stopband Range," *IEEE Transactions on Microwave Theory and Techniques*, Vol. 55, No. 10, Oct. 2007.

[3] Weng, M.-H., C.-Y. Hung, and Y.-K. Su, "A Hairpin Line Diplexer For Direct Sequence Ultra-Wideband Wireless Communications," *IEEE Microwave and Wireless Components Letters*, Jul. 2007, Vol. 17, No. 7.

[4] Zong, B. F., Wang, G. M., Zeng, H. Y., & Wang, Y. W. (2012). Compact and High Performance Dual-band Bandpass Filter using Resonator-embedded Scheme for WLANs. *Radioengineering*, 2012, vol. 21(4), pp. 1051.

[5] Mo, S.-G., Z.-Y. Yu, and L. Zhang, "Design of Triple-Mode Bandpass Filter Using Improved Hexagonal Loop Resonator," *Progress In Electromagnetics Research,* 2009, vol. 96, pp. 117–125.

[6] Adam, H., A. Ismail, M. A. Mahdi, M. S. Razalli, A. Alhawariand, and B. K. Esfeh, "X-Band Miniaturized Wideband Bandpass Filter Utilizing Multilayered Microstrip Hairpin Resonator," *Progress In Electromagnetics Research*, 2009, vol. 93, pp. 177–188.

[7] Worapishet, A., Srisathit, K., & Surakampontorn, W. (2012). Stepped-Impedance Coupled Resonators For Implementation of Parallel Coupled Microstrip Filters With Spurious Band Suppression. *Microwave Theory and Techniques, IEEE Transactions on*, 2012, vol. 60(6), pp. 1540-1548.

[8] Hsu, C. L., Hsu, F. C., & Kuo, J. T. (2005, June). Microstrip Bandpass Filters For Ultra-Wideband (UWB) Wireless Communications. *In Microwave Symposium Digest, 2005 IEEE MTT-S International*, 2005, pp. 4.

[9] Abbosh, A. M. "Design Method For Ultra-Wideband Bandpass Filter With Wide Stopband Using Parallel-Coupled Microstrip Lines." *Microwave Theory and Techniques, IEEE Transactions on*, 2012, vol. 60(1), pp. 31-38.

[10] Shaman, H., & Hong, J. S. (2006, December). "An Optimum Ultra-Wideband (UWB) Bandpass Filter With Spurious Response Suppression." *In Wireless and Microwave Technology Conference, 2006. WAMICON'06. IEEE Annual*, 2006, pp. 1-5.

[11] Tan, X., Jin, B., & Zhang, R. Well-Designed Of UWB Suspended Substrate Stripline Highpass Filters. *In 2010 IEEE International Conference on Ultra-Wideband*, 2010, vol. 2, pp. 1-3.

[12] Pirani, S., Nourinia, J., and Ghobadi, C. "Band-Notched UWB BPF Design Using Parasitic Coupled Line," *IEEE Microwave and Wireless Components Letters*, 2010, vol. 20, no. 8, pp. 444-446.

[13] Pierre J. and Jacques B., *Advanced Design Techniques and Realizations of Microwave and RF Filters*, New Jersey: John Wiley & Sons, 2008.

[14] Menzel, W., and Al-Attari, J., Suspended Stripline Filters Integrated with Standard Multilayer Printed Circuit Boards. *2009 German Microwave Conference*, 2009, pp. 1-4.

[15] Hong, J. S., *Microstrip Filters for RF/Microwave Applications, 2nd ed.*, New Jersey: John Wiley & Sons, 2011.

[16] Hunter, I.C., *Theory and Design of Microwave Filter*, London: Institution of Electrical Engineers, 2001.

[17] Zakaria, Z., Mutalib, M. A., Isa, M. S. M., Md. Isa, A. A., Zainuddin, N. A., and Sam, W. Y. "Design of Generalized Chebyshev Lowpass Filter with Defected Stripline Strucuture (DSS)," *IEEE Symposium on Wireless Technology and Applications (ISWTA)*, 2013, pp. 230-235.